



## UvA-DARE (Digital Academic Repository)

### Aspects of photodetection in cervical and ovarian neoplasia

Aalders, M.C.G.

**Publication date**  
2001

[Link to publication](#)

#### **Citation for published version (APA):**

Aalders, M. C. G. (2001). *Aspects of photodetection in cervical and ovarian neoplasia*. [Thesis, fully internal, Universiteit van Amsterdam].

#### **General rights**

It is not permitted to download or to forward/distribute the text or part of it without the consent of the author(s) and/or copyright holder(s), other than for strictly personal, individual use, unless the work is under an open content license (like Creative Commons).

#### **Disclaimer/Complaints regulations**

If you believe that digital publication of certain material infringes any of your rights or (privacy) interests, please let the Library know, stating your reasons. In case of a legitimate complaint, the Library will make the material inaccessible and/or remove it from the website. Please Ask the Library: <https://uba.uva.nl/en/contact>, or a letter to: Library of the University of Amsterdam, Secretariat, P.O. Box 19185, 1000 GD Amsterdam, The Netherlands. You will be contacted as soon as possible.

## Chapter 5

# A mathematical evaluation of dose dependent PpIX fluorescence kinetics *in vivo*

Maurice Aalders, Nine van der Vange, Willem Star, Dick Sterenberg.

*Photochemistry and Photobiology*, 2001, **74(2)**, in press

## **Abstract**

*In vivo* pharmacokinetics of protoporphyrin IX (PpIX) after administration of aminolevulinic acid (ALA) cannot be described accurately by mathematical models using first order rate processes. We have replaced first order reaction rates (fixed time constants) by dose dependent (Michaelis-Menten) reaction rate constants in a mathematical compartment model. Different combinations of first order and dose dependent reaction rates were evaluated to see which one would improve the goodness of fit to experimentally determined *in vivo* PpIX fluorescence kinetics as a function of concentration. The mathematical models that were evaluated are all based on a three-compartment model for the drug distribution, conversion to PpIX and subsequent conversion to heme. Implementation of dose dependent reaction rates improved the goodness of fit and enabled interpolation to other drug doses. For most data sets, the time constant for delivery to the target cells turned out to be dose dependent. For all data sets, use of Michaelis-Menten rates for the conversion of ALA to PpIX yielded better fits. The clearance of PpIX turned out to be a first order process for all doses and types of administration. Fluorescence curves measured on a specific tissue type but obtained in different studies with different measurement techniques could be described with one single set of parameters.

## Introduction

Photodynamic therapy and photodetection are based on differences in concentration of photosensitizing drugs in neoplastic tissues versus their host tissue<sup>1,2</sup>. This implies the importance of accurate pharmacokinetics to identify the period of maximum concentration differences. In general, pharmacokinetics of fluorescent drugs depends on type of drug, type of tissue, application period and drug dose. These parameters all determine the optimal time for treatment or diagnostics.

Currently, protoporphyrin IX (PpIX) is the most widely used fluorescent photosensitizer in oncology. PpIX is formed from its precursor 5-aminolevulinic acid (ALA). After distribution through the body ALA is converted in the cells to PpIX via a number of sequential chemical reactions. These conversion steps are enzyme controlled and therefore rate limited<sup>3</sup>. As a consequence the rate of increase and maximum intensity of fluorescence emission is not linearly related to the applied quantity of the precursor.

First order mathematical kinetic models are generally used to extract time constants, which describe the rate of conversion from ALA to PpIX and the consecutive conversion of protoporphyrin IX to heme<sup>4-8</sup>. Especially when higher drug doses are used the fit to the experimental data is not satisfactory. Furthermore, using a first order kinetic model no extrapolations can be made to other drug doses because of the absence of dose dependency in the equations. This limits the utility of the model as for each drug dose a new series of experiments has to be performed.

A more realistic description of PpIX pharmacokinetics could possibly be obtained by using a mathematical model based on Michaelis-Menten (MM) kinetics. MM is used in biochemistry to calculate enzyme-controlled reactions<sup>9</sup>. The MM approach takes the dose dependency of the enzyme controlled conversion (reaction) rate into account. With this model the full relationship between PpIX kinetics and ALA dose may be obtained.

After administration of ALA, the intermediate compound that has the lowest conversion rate will accumulate. Hua *et al.*<sup>3</sup> showed that the amount of PpIX accumulated *in vivo* increases with increasing ALA administration until the enzymes have reached their maximum turnover capacity causing the amount of accumulated PpIX to level off. Rate limited reactions like this may be more accurately described using MM reaction rate constants<sup>9</sup>. In the mathematical models that we are proposing, we have replaced first order time constants of a three-compartment model by dose dependent (MM) reaction

rates. Different combinations of dose dependent and dose independent reaction rates constants were evaluated to assess the best mathematical description. Furthermore, we evaluated the possibility to use one set of parameters for multiple ALA doses. We fitted the mathematical models to data obtained from earlier studies in which we measured PpIX pharmacokinetics in various mammals after administration of different doses of ALA<sup>10</sup>. In addition, we fitted the model to clinical data obtained from several published studies on pharmacokinetics of ALA induced PpIX<sup>5,11,12</sup>.

## Methods

**Three-compartment model** The mathematical equations are based on a three-compartment model previously published in the literature by several authors<sup>5-7</sup> which represents the essential parts of the bio-synthetic pathway of heme (figure 1). For each compartment we will derive a rate equation.

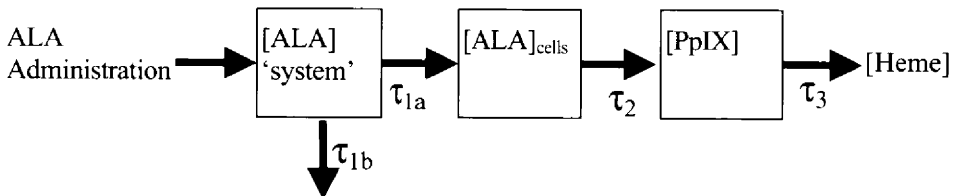


Figure 1 : schematic picture of the simplified bio-synthetic pathway of heme.

After administration ALA is either excreted directly ( $\tau_{1b}$ ) (for systemic administration this means through the renal pathway) or transported to the target cells ( $\tau_{1a}$ ). The rate equation for the first compartment becomes:

$$\frac{\partial [ALA]_{system}}{\partial t} = -\frac{[ALA]_{system}}{\tau_{1a}} - \frac{[ALA]_{system}}{\tau_{1b}} = -\frac{[ALA]_{system}}{\tau_1} \quad (1)$$

$$\frac{1}{\tau_1} = \frac{1}{\tau_{1a}} + \frac{1}{\tau_{1b}}$$

Only time constant  $\tau_{1a}$  will follow from the modeling procedures.

The ALA fraction that is transported to and accumulates at the cellular site ( $[ALA]_{cells}$ ) is subsequently converted with reaction rate  $1/\tau_2$ , to PpIX which is the next step in the model. We assume that the conversion from exogenous ALA is the sole source for PpIX, which results in a concentration  $[PpIX]$ . The clearance of PpIX from the cells is caused

by the transformation of PpIX into heme ( $\tau_3$ ). It is assumed that the contribution of circulating porphyrins is negligible. For these two compartments the rate equations are

$$\frac{\partial [ALA]_{cells}}{\partial t} = + \frac{[ALA]_{system}(t)}{\tau_{1a}} - \frac{[ALA]_{cells}(t)}{\tau_2} \quad (2)$$

and

$$\frac{\partial [PpIX]}{\partial t} = + \frac{[ALA]_{cells}(t)}{\tau_2} - \frac{[PpIX](t)}{\tau_3} \quad (3)$$

As mentioned before, the time constants,  $\tau_1, \tau_2$  and  $\tau_3$  are either fixed time constants or dose dependent (inverse) Michaelis-Menten reaction rates. This 'Michaelis-Menten' time constant, as described in equation 4, will be substituted in equation 2 and/or 3.

$$\tau_{michaelis-menten} = \frac{[ALA]_{Cells} + K_m}{V_{max}} \quad (4)$$

Where  $V_{max}$  is the maximum ALA to PpIX conversion rate and the  $K_m$  is the Michaelis-Menten constant.

The Michaelis-Menten ( $K_m$ ) constant is a measure for the affinity of an enzyme for its substrate, the  $V_{max}$  is a measure of the enzyme activity. In case of low ALA concentrations, the dose dependency of  $\tau_2$  is absent and only the ratio of the  $K_m$  and  $V_{max}$  can be determined, not their individual values. In addition to the time constants  $\tau_1, \tau_2$  and  $\tau_3$  some authors include factors to correct for the losses of ALA to the renal pathway, to other tissues before reaching target cells and the losses due to the uptake of the ALA by the target tissue<sup>6</sup>. In the fitting procedure we add only one extra factor to describe the relationship between the PpIX concentration and the measured quantity (= fluorescence in the datasets that were used in this manuscript), which may be different between different data sets used.

Three models will be tested on experimental data in order to assess the best mathematical description of the time and dose dependent build-up and clearance of PpIX. Various different fluorescence measurement techniques and devices have been used for the experiments quoted in this paper. We assume all these measurements to yield a quantity proportional to the tissue PpIX concentration. This proportionality constant is unknown and is estimated in the fitting procedure. The  $\chi^2$ -test is used to evaluate the goodness of

fit. The result of the  $\chi^2$  test will be expressed in  $\chi^2$  per degree of freedom (reduced  $\chi^2$ ). The F-test<sup>13</sup> is used to evaluate whether the addition of an extra fitting parameter significantly improves the goodness of fit.

**1st model** : only first order time constants The first proposed model uses three first order time constants. This is the classical approach. We include this in the study for comparative reasons.

**2nd model** : Michaelis-Menten rate constants for  $\tau_2$  For this model a dose dependent reaction rate to describe the conversion of ALA to PpIX was introduced ( $\tau_2$ ). For the distribution of ALA ( $\tau_1$ ) and the clearance of PpIX, ( $\tau_3$ ), first order time constants are maintained.

**3rd model** : MM for  $\tau_2$  and  $\tau_3$  The next logical step is to also replace the PpIX to heme (constant) reaction rate ( $\tau_3$ ) by a PpIX dose dependent MM-type rate. From the literature we know that this reaction is also enzyme controlled<sup>3</sup>. However, it is unknown whether the usual ALA induced PpIX concentrations are high enough for the reaction rate to become dose dependent.

**4th model**: MM for  $\tau_1$  and  $\tau_2$  In this set of equations, MM kinetics are used in both the distribution of ALA ( $\tau_1$ ) and in the conversion of ALA to PpIX ( $\tau_2$ ). For the clearance of PpIX, ( $\tau_3$ ), a first order time constant is maintained. The use of MM kinetics for  $\tau_1$  might be relevant for the description of rate limited distribution of ALA. In systemic application, we expect  $1/\tau_{1a}$  to be much smaller than  $1/\tau_{1b}$ , i.e. the bulk of the ALA does not go to the target tissue but elsewhere depending on the tissue type. In case of topical administration on the skin the ALA has to diffuse through the target tissue (the skin) to reach the vasculature. Hence, we expect  $1/\tau_{1a}$  to be much larger than  $1/\tau_{1b}$ , i.e. most of the ALA goes to the target tissue. This dominant transport might be rate limited.

#### **Data to be analyzed.**

Our models were fitted to the data obtained from a previously reported rat study performed in our group and data obtained from other studies available in the literature (specified below). In the figures the unit 'apparent concentration' is used. No absolute comparison can be made between the absolute values in the different graphs. We will only obtain time constants  $\tau$  or the ratio  $K_m/V_{max}$  which also has the dimension of time.

### Rat kinetics experiments

Earlier, we performed an animal study in which we investigated the pharmacokinetics of protoporphyrin IX in the abdominal cavity of tumor bearing rats after intravenous administration of different doses of ALA. PpIX kinetics was assessed using *in vivo* fluorescence measurement for up to 24 hours on liver, intestines and skin. Details concerning these experiments are reported in chapter 4<sup>10</sup>.

### Experiments published in the literature

We used PpIX fluorescence kinetics as obtained in three studies from the literature. In a mouse study by van den Akker *et al.*<sup>12</sup>, ALA was applied topically on the skin in doses ranging from 1% to 40% solution (w/w).

In addition data from Rhodes *et al.*<sup>11</sup> were used. The authors measured PpIX kinetics after iontophoretically controlled administration of ALA in the healthy skin of human volunteers. Measurements on healthy human forearm by Rick *et al.*<sup>5</sup> were compared with (unpublished) data that were obtained in our institute to see whether data obtained of different studies could be described with one set of fit parameters.

## Results

Figure 2 shows PpIX fluorescence kinetics as obtained in a mouse study by van den Akker *et al.*<sup>12</sup> In this study ALA was applied topically on the skin in doses ranging from 1% to 40% solution (w/w). The dependency of the shape of the curves on the ALA dose is clearly observable. The time of maximum fluorescence increases with increasing ALA dose. The four mathematical models were fitted to these curves. The fit of model 1 to the data resulted in a reduced  $\chi^2$  of 5.17 (27 deg of freedom, not acceptable  $p < 0.05$ ). The fact that the  $\chi^2$  fit gives a result that is statistically not acceptable illustrates the need for a more sophisticated model. Model 2 resulted in a reduced  $\chi^2$  of 1.32 (26 deg of freedom) which is an acceptable fit. Model 3 produces a reduced  $\chi^2$  of 1.37 (at 25 degrees of freedom), also an acceptable fit, but the introduction of the dose dependent time constant  $\tau_3$  did not give a significant improvement in the goodness of fit (F-test). This suggests that the PpIX concentration is below the saturation level in the conversion of PpIX to Heme. Model 4 yields a reduced  $\chi^2$  of 1.13, at 25 degrees of freedom. This is a significant increase in the goodness of fit. The lines in figure 2 represent the fit of model 4 to the experimental data. The fitting parameters for each model are summarized in table 1.

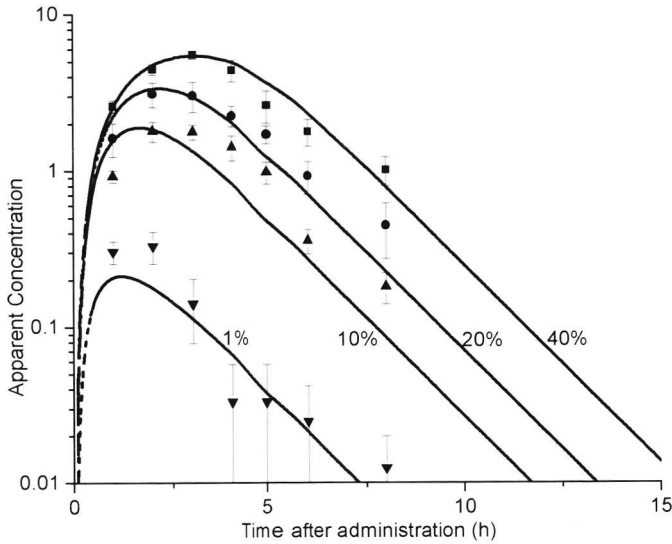


Figure 2: In vivo PpIX fluorescence kinetics in mouse skin after topical application of 1, 10, 20 and 40% ALA solution. The lines represent the fit of mathematical model 4 to the experimental data.

Figure 3 shows the experimental data as published by Rhodes *et al.*<sup>11</sup> ALA was applied iontophoretically to the skin of healthy volunteers. The amount of applied ALA was assumed to be proportional to the applied charge (in mC). The fit of model 1 resulted in a reduced  $\chi^2$  of 3.73 (31 degrees of freedom) which is not acceptable. Models 2 and 3 gave both acceptable ( $p < 0.05$ ) results (reduced  $\chi^2$  of 1.61 and 1.24 respectively). As in figure 1,  $\tau_1$  turned out to have a dose dependency. So, again, model 4 yielded the best result. (reduced  $\chi^2 = 0.95$ , 29 deg of freedom. For the  $\chi^2$  calculation, a standard deviation of 20 % of the value of the data points was assumed). This was significantly better

Table 1: Fit parameters from fitting the four mathematical models on the experimentally determined PpIX fluorescence kinetics in kinetics in mouse skin after topical application of 1, 10, 20 and 40 % ALA solution. The columns give the time constants for the distribution of ALA to the target cells, the conversion of ALA to PpIX and the consecutive conversion of PpIX to heme. When a first order equation is used, a single  $\tau$  is given. The arrows indicate whether the addition of an extra fit parameter improves the goodness of fit significantly.

	ALA <sub>system</sub> ⇒ ALA-cells		ALA <sub>cells</sub> ⇒ PpIX		PpIX ⇒ Heme		Goodness of fit Reduced $\chi^2$ ; (deg of freedom)	F-test
	$K_m$ $\tau$ (hours)	Vmax	$K_m$ $\tau$ (hours)	Vmax	$K_m$ $\tau$ (hours)	Vmax		
<b>Model 1</b>	1.21		1.10		1.23		5.17 ; (27)	* * *
<b>Model 2</b>	0.29		2.34	4.72	0.56		1.32 ; (26)	
<b>Model 3</b>	0.33		2.36	4.72	68	39	1.37 ; (25)	
<b>Model 4</b>	<b>1.77</b>	<b>16.21</b>	<b>4.28</b>	<b>6.25</b>	<b>1.74</b>		<b>1.13 ; (25)</b>	

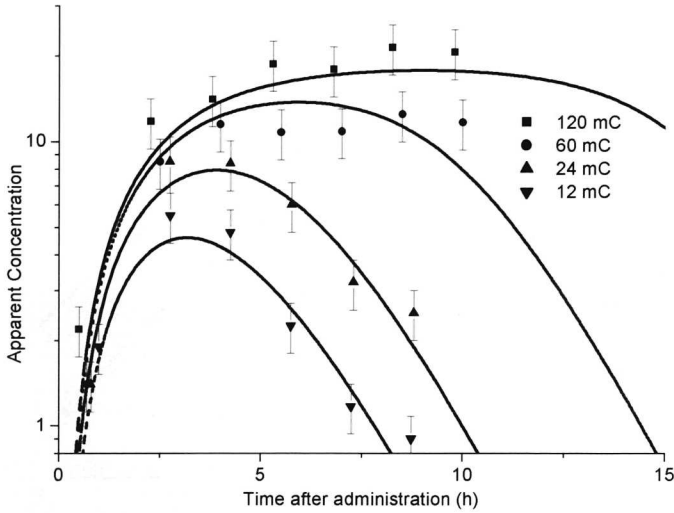


Figure 3: data of Rhodes *et al.*<sup>11</sup> Fluorescence measurements on human skin after iontophoretic administration of ALA. The lines represent the fit of mathematical model 4 to the experimental data.

than the other models (F-test). The fitting parameters for each model are summarized in table 2. In figure 3, the lines represent the fit of model 4 to the experimental data. The data points represent measurements on a single volunteer.

For figure 4 we took data from an article by Rick *et al.*<sup>5</sup> which showed the results of fluorescence measurements on human forearm after administration of 40 mg/kg ALA. In addition, we used data that we obtained from studies that we performed in our institute

Table 2 : Fit parameters from fitting the four mathematical models on the experimentally determined PpIX fluorescence kinetics on human skin after iontophoretic administration of ALA.

The columns give the time constants for the distribution of ALA to the target cells, the conversion of ALA to PpIX and the consecutive conversion of PpIX to heme. When a first order equation is used, a single  $\tau$  is given. The arrows indicate whether the addition of an extra fit parameter improves the goodness of fit significantly.

	ALA <sub>system</sub> ⇒ ALA-cells		ALA <sub>cells</sub> ⇒ PpIX		PpIX ⇒ Heme		Goodness of fit Reduced $\chi^2$ ; (deg of	F-test
	K <sub>m</sub>	V <sub>max</sub>	K <sub>m</sub>	V <sub>max</sub>	K <sub>m</sub>	V <sub>max</sub>		
	$\tau$ (hours)		$\tau$ (hours)		$\tau$ (hours)			
Model 1	1.99		1.99		1.99		3.73 ; (31)	*
Model 2	1.43		6.30	7.59	2.27		1.61 ; (30)	
Model 3	1.60		7.64	7.82	19.39	12.05	1.24 ; (29)	*
Model 4	<b>18.01</b>	<b>16.37</b>	<b>29.42</b>	<b>26.31</b>	<b>1.42</b>		<b>0.95 ; (29)</b>	

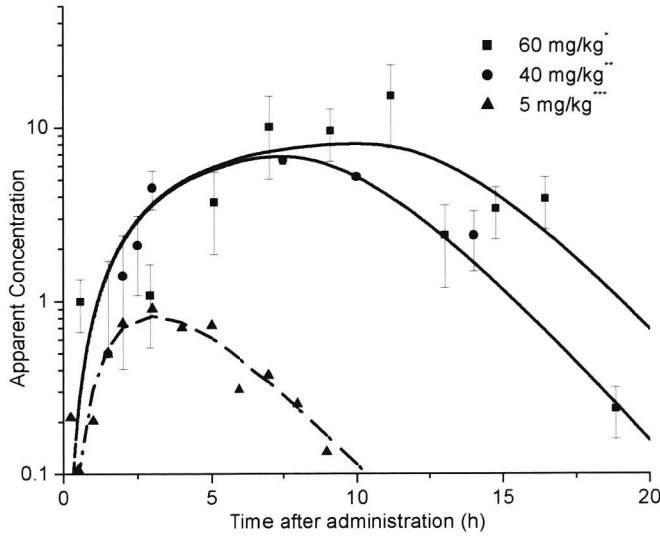


Figure 4: \* Measurements performed in our group on forearm of 5 healthy volunteers, \*\* measurements on forearm of healthy volunteers by K. Rick *et al*, \*\*\* Measurements performed in our group on forearm of patients. The lines represent the fit of mathematical model 4 to the experimental data.

using 5 and 60 mg/kg. An extra fit parameter was defined to adjust the amplitude of the measurements of Rick *et al*. The fit of model 1 resulted in a reduced  $\chi^2$  of 3.87 (31 degrees of freedom) which is not acceptable. Models 2 and 3 gave both significant results (reduced  $\chi^2$  of 0.97 and 0.96 respectively :  $p < 0.05$ ).  $\tau_1$  turned out to have a dose dependency. The fitting parameters for each model are summarized in table 3. model 4 yielded significantly the best result (reduced  $\chi^2 = 0.86$ , 29 deg of freedom)

Table 3 : Fit parameters from fitting the four mathematical models on the experimentally determined PpIX fluorescence kinetics in human forearm after oral administration of 5, 40 and 60 mg/kg ALA. The columns give the time constants for the distribution of ALA to the target cells, the conversion of ALA to PpIX and the consecutive conversion of PpIX to heme. When a first order equation is used, a single  $\tau$  is given. The arrows indicate whether the addition of an extra fit parameter improves the goodness of fit significantly.

	ALA <sub>system</sub> ⇒ ALA <sub>cells</sub>		ALA <sub>cells</sub> ⇒ PpIX		PpIX ⇒ Heme		Goodness of fit Reduced $\chi^2$ ; (deg of freedom)	F-test
	K <sub>m</sub>	V <sub>max</sub>	K <sub>m</sub>	V <sub>max</sub>	K <sub>m</sub>	V <sub>max</sub>		
	$\tau$ (hours)		$\tau$ (hours)		$\tau$ (hours)			
Model 1	0.14		1.57		1.64		3.87 ; (31)	* ←
Model 2	1.02		15.72	23.55	3.28		0.97 ; (30)	
Model 3	0.84		16.35	3.89	1.32	6.83	0.96 ; (29)	
<b>Model 4</b>	<b>2.33</b>	<b>6.49</b>	<b>20.06</b>	<b>10.72</b>	<b>2.10</b>		<b>0.86 ; (29)</b>	* ←

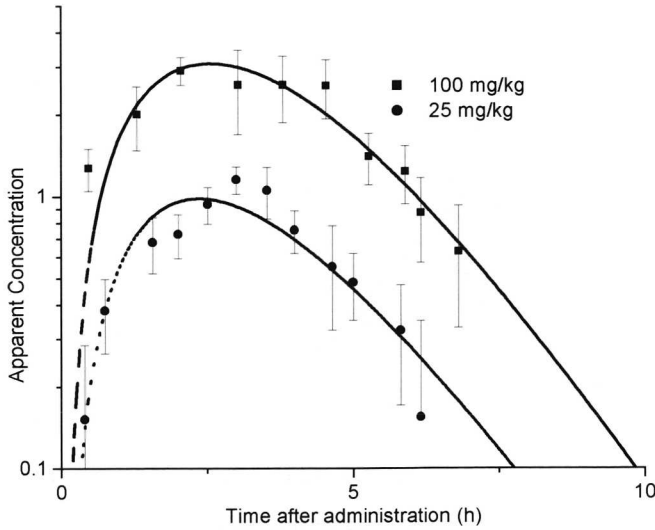


Figure 5: PpIX kinetics in the rat small intestine after i.p. administration of 25 and 100 mg/kg ALA<sup>10</sup>. The symbols represent actual measured fluorescence data points while the lines represent the MM fit of model 2 for the different doses of ALA.

Figure 5 shows the time dependent PpIX fluorescence in rat small intestine after intra-peritoneal (i.p.) administration of 25 and 100 mg/kg ALA<sup>10</sup>. The dependency of the shape of the curves on the ALA dose is not so obvious in this example. This resulted in a small variation in the goodness of fit for the different models.(see table 4). Use of model 2 resulted in the best reduced  $\chi^2$  of 0.83 (deg of freedom : 24).

Table 4 : Fit parameters from fitting the four mathematical models on the experimentally determined PpIX fluorescence kinetics in the rat small intestine after i.p. administration of 25 and 100 mg/kg ALA. The columns give the time constants for the distribution of ALA to the target cells, the conversion of ALA to PpIX and the consecutive conversion of PpIX to heme. When a first order equation is used, a single  $\tau$  is given. The arrows indicate whether the addition of an extra fit parameter improves the goodness of fit significantly.

	ALA <sub>system</sub> ⇒ ALA <sub>cells</sub>		ALA <sub>cells</sub> ⇒ PpIX		PpIX ⇒ Heme		Goodness of fit Reduced $\chi^2$ ; (deg of freedom)	F-test
	K <sub>m</sub>	Vmax	K <sub>m</sub>	Vmax	K <sub>m</sub>	Vmax		
	$\tau$ (hours)		$\tau$ (hours)		$\tau$ (hours)			
Model 1	1.20		1.22		1.23		0.85 ; (25)	
Model 2	<b>1.31</b>		<b>17.11</b>	<b>15.03</b>	<b>0.97</b>		<b>0.83 ; (24)</b>	
Model 3	1.26		15.05	13.35	84	82	0.96 ; (24)	
Model 4	166	162	27	16	1.48		0.95 ; (23)	

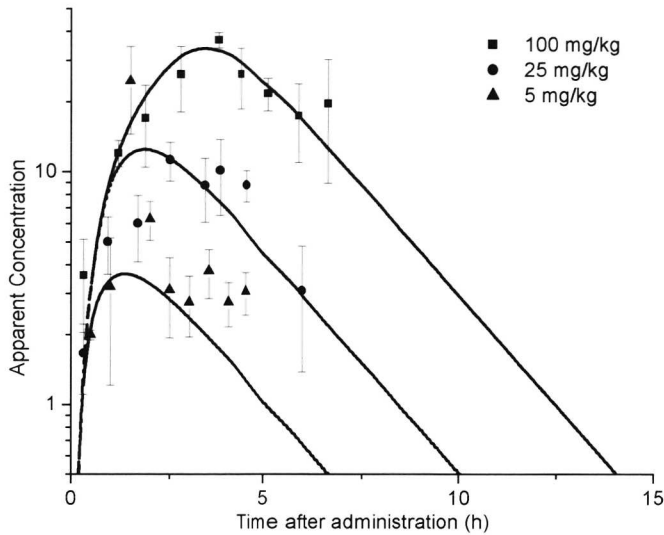


Figure 6: PpIX fluorescence kinetics measured on rat liver after i.p. administration of 5, 25 and 100 mg/kg ALA(10). The symbols represent actual measured fluorescence data points while the lines represent the MM fit of model 4 for the different doses of ALA.

Figure 6 shows the time dependent profile of PpIX fluorescence in rat liver after i.p. administration of 5, 25 and 100 mg/kg ALA<sup>10</sup>. In this example, the fluorescence data points obtained with 5 mg/kg are relatively high compared to the curve obtained from the model fit. Model 4 yielded the best fit (significant, reduced  $\chi^2 = 1.04$ , deg of freedom : 30) suggesting that transport of ALA to the liver may be rate limited. Models 2 and 3 resulted also in a significant fit ( $p < 0.05$ , reduced  $\chi^2 = 1.41$  and 1.39, deg of freedom : 31 and 30). The fitting parameters for each model are summarized in table 5.

Table 5 : Fit parameters from fitting the four mathematical models on the experimentally determined PpIX fluorescence kinetics on rat liver after i.p. administration of 5, 25 and 100 mg/kg ALA. The columns give the time constants for the distribution of ALA to the target cells, the conversion of ALA to PpIX and the consecutive conversion of PpIX to heme. When a first order equation is used, a single  $\tau$  is given. The arrows indicate whether the addition of an extra fit parameter improves the goodness of fit significantly.

	ALA <sub>system</sub> ⇒ ALA-cells		ALA <sub>cells</sub> ⇒ PpIX		PpIX ⇒ Heme		Goodness of fit	F-test
	K <sub>m</sub>	V <sub>max</sub>	K <sub>m</sub>	V <sub>max</sub>	K <sub>m</sub>	V <sub>max</sub>		
	$\tau$ (hours)		$\tau$ (hours)		$\tau$ (hours)		Reduced $\chi^2$ ; (deg of freedom)	
Model 1	2.17		3.92		2.20		9.57 ; (32)	*
Model 2	0.15		9.81	16.04	1.54		1.41 ; (31)	
Model 3	0.11		7.93	14.20	65	26	1.39 ; (30)	*
<b>Model 4</b>	<b>1.34</b>	<b>26.89</b>	<b>37</b>	<b>55</b>	<b>2.38</b>		<b>1.04 ; (30)</b>	

Model 1 resulted in an unsatisfactory fit ( $\chi^2 = 9.57$ , deg of freedom : 32).

## Discussion

In this paper we evaluated several refinements in the mathematical description of the time dependent *in vivo* synthesis and clearance of the fluorescent protoporphyrin IX after administration of 5-aminolevulinic acid (ALA). The complex system of the distribution of ALA, the subsequent conversion of ALA to PpIX and the clearance of PpIX are simplified to a three compartment mathematical model. Such models, usually incorporating first order reaction rates can be found in several published studies. The fixed time constant approach does not yield curves that fit satisfactorily for a range of different ALA doses. For this reason we substituted the first order reaction rate constants for ALA dose dependent reaction rate constants described by Michaelis-Menten (MM) kinetics. This yielded much better results. Several combinations of first order time constants and MM constants were evaluated.

The mathematical models were validated using *in vivo* fluorescence data obtained on both humans and animals. For our validation we required a set of measurements using at least 2 different ALA doses and in a wide time range to accurately describe both the increase in PpIX and the decrease. Such data sets are rarely found in the literature. The most common problem was the lack of data points distributed throughout the curve or intervention by therapy. The conversion of PpIX to heme turned out to be best described by first order kinetics, indicating a reaction that remains below its saturation level.

PpIX Fluorescence kinetics that were obtained after topical administration, turned out to have a dose dependent distribution rate of ALA. The rate of passive diffusion is not dose dependent. The dose dependency for the distribution rate suggests active transport mechanisms to dominate transport through the skin. Most likely the bottleneck for the hydrophilic ALA to move through the epidermis is formed by the cell membranes. Although the ALA transport through membranes is not an enzymatic reaction as described by the Michaelis-Menten equation, it does require the intervention of carrier proteins. Here the proteins are transport rate limiting and may therefore induce a dose dependent rate similar to enzyme reaction rates. PpIX Fluorescence kinetics that were obtained on rat liver after systemic administration, turned out to also have a dose dependent distribution rate of ALA (figure 6). The fact that introduction of a dose dependent  $\tau_1$  in the fluorescence measurements on rat intestine after systemic administration of ALA (Figure 5) did not significantly improve the fit suggests that in this case

either passive diffusion plays a dominant role or the active transport mechanisms responsible for systemic removal of ALA are operating far below their rate limits.

In all cases, the replacement of the ALA to PpIX (dose independent) reaction rate by a ALA dose dependent MM-type rate improved the fit to the experimental data. The liver turned out to have the highest  $K_m$  and  $V_{max}$  for the conversion of ALA to PpIX. The enzyme activity for the ALA to PpIX conversion in the intestine was about one third of that found in liver. This might explain the higher porphyrin concentration usually found in liver<sup>10</sup>. The relation between porphyrin accumulation and enzyme activity was studied by Hua *et al.*<sup>3</sup> who assessed the activity of ferrochelatase and porphobilinogen deaminase, two key enzymes in the bio-synthetic heme pathway. They concluded that there is no simple relationship apparent between the activities of these enzymes and the concentration of porphyrins in the different tissues.

The replacement of the PpIX to heme (first order) reaction rate by a PpIX dose dependent MM-type rate did not appear to be useful. This suggests that the enzymes responsible for the breakdown of PpIX are present in sufficient abundance for all PpIX doses occurring in this study, and a PpIX dose dependency as described by MM kinetics may occur at much higher PpIX doses. From a biological point of view this makes sense, as PpIX presents danger to cells that produce it and it has no purpose in itself. It would be interesting to see if the same  $K_m$  would be found in porphyric patients.

In general, the experimentally determined fluorescence kinetics curves could be described more accurately with the MM models compared to the first order mathematical model. A comparison of actual measured fluorescence data points and the curve of the MM fit indicates the validity of MM kinetics in PpIX fluorescence pharmacokinetics. This holds for the curves that were used in this paper. The hypothesis that the MM model may be used to inter- and extrapolate to other drug doses seems to be valid. For confirmation of the conclusions arrived at in this paper, more kinetic experiments will have to be performed.

## Acknowledgements

The authors would like to thank Fiona Stewart of the Netherlands Cancer Institute in Amsterdam for her help on various aspects of this manuscript.

## References

1. J.C. Kennedy, R.H. Pottier, D.C. Pross, Photodynamic therapy with endogenous protoporphyrin IX: basic principles and present clinical experience. *J. Photochem. Photobiol. B*, 1990, **8**, 143-148.
2. J.C. Kennedy, R.H. Pottier, Endogenous protoporphyrin IX, a clinically useful photosensitizer for photodynamic therapy. *J. Photochem. Photobiol. B*, 1992, **14**, 275-292.
3. Z. Hua, S.L. Gibson, T.H. Foster, R. Hilf, Effectiveness of d-aminolevulinic acid-induced protoporphyrin as a photosensitizer for photodynamic therapy *in vivo*. *Cancer Res.* 1995, **55**, 1723-1731.
4. R. Sroka, W. Beyer, L. Gossner, T. Sassy, S. Stocker, R. Baumgartner, Pharmacokinetics of 5-aminolevulinic-acid-induced porphyrins in tumor-bearing mice. *J. Photochem. Photobiol. B*, 1995, **34**, 13-19.
5. K. Rick, R. Sroka, H. Stepp, M. Kriegmair, R.M. Huber, K. Jacob, R. Baumgartner, Pharmacokinetics of 5-aminolevulinic acid-induced protoporphyrin IX in skin and blood. *J. Photochem. Photobiol. B* 1997, **40**, 313-319.
6. C. Abels, P. Heil, M. Dellian, G.E.H. Kuhnle, R. Baumgartner, A. Götz, *In vivo* kinetics and spectra of 5-aminolevulinic acid induced fluorescence in an amelanotic melanoma of the hamster, *Br. J. Cancer* 1995, **70**, 826-833.
7. V.V. Vaidyanathan, S. Rastegar, T.W. Fossum, P. Flores, E.W.J. van der Breggen, N.G. Egger, S.L. Jacques, M. Motamedi, A study of aminolevulinic acid-induced protoporphyrin IX fluorescence kinetics in the canine oral cavity, *Lasers Surg. Med.*, 2000, **26**, 405-414.
8. L.O. Svaasand, P. Wyss, M.-T. Wyss, Y. Tadir, B.J. Tromberg, M.W. Berns Dosimetry model for photodynamic therapy with topically administered photosensitizers. *Lasers Surg. Med.*, 1996, **18**, 139-149.
9. P.W. Atkins, *The rates of chemical reactions. Physical Chemistry*, ed. 1992, pp. 777-813, Oxford University Press, Oxford.
10. M.C.G. Aalders, H.J.C.M. Sterenborg, F.A. Stewart, N. van der Vange Photodetection with 5-aminolevulinic acid induced protoporphyrin IX in the rat abdominal cavity: drug dose dependent fluorescence kinetics. *Photochem. Photobiol.*, 2000, **72**, 521-525.
11. L.E. Rhodes, M.M. Tsoukas, R.R. Anderson, N. Kollias, Iontophoretic delivery of ALA provides a quantitative model for ALA pharmacokinetics and PpIX phototoxicity in human skin. *J. Invest. Derm.*, 1997, **108**, 87-91.
12. J.T. van den Akker, H.S. Bruijn, G.M. Beijersbergen van Henegouwen, W.M. Star, H.J.C.M. Sterenborg, protoporphyrin IX fluorescence kinetics and localization after topical application of ALA pentyl ester and ALA on hairless mouse skin with UVB-induced early skin cancer, *Photochem. Photobiol.*, 2000, **72**, 399-406.
13. Bevington, R. and D.K. Robinson, *Data reduction and error analysis for the physical sciences*, McGraw-Hill, 1992, New York.

